Neutron Matter at Next-to-Next-to-Next-to-Leading Order in Chiral Effective Field Theory

I. Tews, T. Krüger, K. Hebeler, and A. Schwenk

Neutron matter at next-to-next-to-next-to-leading order in chiral effective field theory

I. Tews,[1,2] T. Krüger,[1,2] K. Hebeler,[3] and A. Schwenk[2,1]

[1]*Institut für Kernphysik, Technische Universität Darmstadt, 64289 Darmstadt, Germany*
[2]*ExtreMe Matter Institute EMMI, GSI Helmholtzzentrum für Schwerionenforschung GmbH, 64291 Darmstadt, Germany*
[3]*Department of Physics, The Ohio State University, Columbus, OH 43210, USA*

Neutron matter presents a unique system for chiral effective field theory (EFT), because all many-body forces among neutrons are predicted to next-to-next-to-next-to-leading order (N^3LO). We present the first complete N^3LO calculation of the neutron matter energy. This includes the subleading three-nucleon (3N) forces for the first time and all leading four-nucleon (4N) forces. We find relatively large contributions from N^3LO 3N forces. Our results provide constraints for neutron-rich matter in astrophysics with controlled theoretical uncertainties.

The physics of neutron matter ranges from universal properties at low densities to the structure of extreme neutron-rich nuclei and the densest matter we know to exist in neutron stars. For these extreme conditions, controlled calculations with theoretical error estimates are essential. Chiral EFT provides such a systematic expansion for nuclear forces [1]. This is particularly exciting for neutron matter and neutron-rich systems, because all three- and four-neutron forces are predicted to N^3LO [2].

Neutron matter based on chiral EFT has been studied using lattice simulations [3] at low densities, $n \lesssim n_0/10$ (with saturation density $n_0 = 0.16\,\text{fm}^{-3}$), and following an in-medium chiral perturbation theory approach [4, 5], where low-energy couplings are adjusted to empirical nuclear matter properties. In addition, the renormalization group (RG) has been used to evolve chiral EFT interactions to low momenta [6], which has enabled perturbative calculations for nucleonic matter [2, 7]. While these constrain the properties of neutron-rich matter to a much higher degree than is reflected in neutron star modeling [8], the dominant uncertainties are due to 3N forces, which were included only to N^2LO. A consistent inclusion of higher-order many-body forces is therefore key.

Here we present the first calculations at nuclear densities based directly on chiral EFT interactions without RG evolution. To this end, we have studied the perturbative convergence of chiral two-nucleon (NN) potentials for neutron matter in detail, and found that the available N^2LO and N^3LO potentials with lower cutoffs $\Lambda = 450 - 500\,\text{MeV}$ are perturbative. This is supported by small Weinberg eigenvalues at low energies indicating the perturbative convergence in the particle-particle channel [6]. In neutron matter, it comes as a result of effective range effects [9], which weaken NN interactions at higher momenta, combined with weaker tensor forces among neutrons, and with limited phase space at finite density due to Pauli blocking [10].

At the NN level we use the N^2LO and N^3LO potentials developed by Epelbaum, Glöckle and Meißner (EGM) [11] with $\Lambda/\widetilde{\Lambda} = 450/500$ and $450/700\,\text{MeV}$ ($\Lambda/\widetilde{\Lambda}$ denotes the cutoff in the Lippmann-Schwinger equation

and in the two-pion-exchange spectral-function regularization, respectively). We also use the $\Lambda = 500\,\text{MeV}$ N^3LO NN potential of Entem and Machleidt (EM) [12], which is most commonly used in nuclear structure calculations. The larger $\Lambda = 550 - 600\,\text{MeV}$ NN potentials of EGM and EM have been found to be nonperturbative [13] and are therefore not included. Moreover, the LO NN contact couplings in the 600/600 and 600/700 EGM potentials break Wigner symmetry perturbatively (at the interaction level), with a repulsive spin-independent C_S
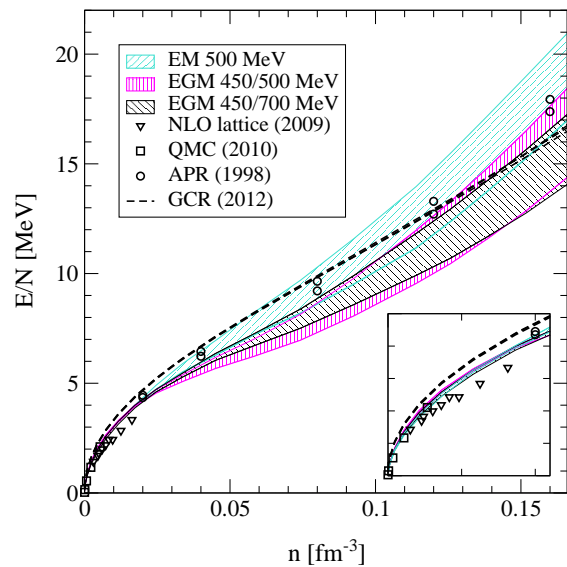

FIG. 1. (Color online) Neutron matter energy per particle as a function of density including NN, 3N and 4N forces at N^3LO. The three overlapping bands are labeled by the different NN potentials and include uncertainty estimates due to the many-body calculation, the low-energy c_i constants and by varying the 3N/4N cutoffs (see text for details). For comparison, results are shown at low densities (see also the inset) from NLO lattice [3] and Quantum Monte Carlo (QMC) simulations [22], and at nuclear densities from variational (APR; the different points are with/without boost corrections) [23] and Auxiliary Field Diffusion MC calculations (GCR) [24] based on adjusted nuclear force models.

and an unnaturally large spin-dependent $C_T \sim C_S$, leading to unexpectedly large C_T-dependent 3N forces.

In this Letter, we include for the first time all N^{3}LO 3N and 4N forces, which have been derived only recently [14–17], in addition to the N^{2}LO 3N forces. Figure 1 shows our complete N^{3}LO calculation of the neutron matter energy as our main result, where the bands include estimates of the theoretical uncertainties due to the many-body calculation and in the many-body forces.

For neutrons, only the two-pion-exchange 3N forces contribute at N^{2}LO [2]. For the corresponding low-energy constants c_1 and c_3, we take the range of values from a high-order analysis [18], at N^{2}LO: $c_1 = -(0.37 - 0.81)\,\text{GeV}^{-1}$ and $c_3 = -(2.71 - 3.40)\,\text{GeV}^{-1}$ (which includes the c_i values in the EGM and EM NN potentials), and when the N^{2}LO 3N forces are included in an N^{3}LO calculation: $c_1 = -(0.75 - 1.13)\,\text{GeV}^{-1}$ and $c_3 = -(4.77 - 5.51)\,\text{GeV}^{-1}$. It has been shown [2] that the N^{2}LO 3N force contributions in neutron matter can be to a good approximation calculated at the Hartree-Fock level. In this first calculation, we therefore evaluate the N^{3}LO 3N and 4N force contributions to the energy per particle E/N at the Hartree-Fock level. The A-body contributions are then given by

$$\frac{E}{N} = \frac{1}{n}\frac{1}{A!} \sum_{\sigma_1,\ldots,\sigma_A} \int \frac{d\mathbf{k}_1}{(2\pi)^3} \cdots \int \frac{d\mathbf{k}_A}{(2\pi)^3}\, f_R^2\, n_{\mathbf{k}_1} \cdots n_{\mathbf{k}_A}$$

$$\times \langle 1\ldots A | \mathcal{A}_A \sum_{i_1 \neq \ldots \neq i_A = 1}^{A} V_A(i_1,\ldots,i_A) | 1\ldots A \rangle, \quad (1)$$

with short-hand notation $i \equiv \mathbf{k}_i \sigma_i$. $\mathcal{A}_A$ denotes the A-body antisymmetrizer and $n_{\mathbf{k}_i} = \theta(k_F - k_i)$ the Fermi-Dirac distributions at zero temperature. We use a Jacobi-momenta regulator; in terms of $\mathbf{k}_i$ given by $f_R = \exp[-((k_1^2 + \ldots + k_A^2 - \mathbf{k}_1 \cdot \mathbf{k}_2 - \ldots - \mathbf{k}_{A-1} \cdot \mathbf{k}_A)/(A\Lambda^2))^{n_{\exp}}]$ with $n_{\exp} = 4$ and 3N/4N cutoff $\Lambda = 2 - 2.5\,\text{fm}^{-1}$. For the nucleon and pion mass, we use $m = 938.92\,\text{MeV}$ and $m_\pi = 138.04\,\text{MeV}$, and for the axial coupling $g_A = 1.29$ and the pion decay constant $f_\pi = 92.4\,\text{MeV}$.

Chiral 3N forces at N^{3}LO can be grouped into

$$V_{3N}^{N^3LO} = V^{2\pi} + V^{2\pi\text{-}1\pi} + V^{\text{ring}} + V^{2\pi\text{-cont}} + V^{1/m}, \quad (2)$$

where we take the long-range parts, the subleading two-pion-exchange, the two-pion–one-pion-exchange and the pion-ring 3N forces, from Ref. [15], and the short-range parts, the two-pion-exchange–contact and relativistic $1/m$-corrections 3N forces from Ref. [16]. In Fig. 2, we give the individual Hartree-Fock contributions to the neutron matter energy. The evaluation is aided because parts of the different 3N force topologies vanish for neutrons, and the results have been checked by two independent calculations. The details of the calculation will be presented in a future paper. At the Hartree-Fock level, the 3N/4N contributions change by $< 5\%$ if the cutoff is

taken to infinity (i.e., $f_R = 1$), but we will also include N^{2}LO 3N forces beyond Hartree-Fock. This requires a consistently used regulator. Estimates of the theoretical uncertainty are provided by varying the 3N/4N cutoff.

The two-pion-exchange 3N forces at N^{3}LO can be largely written as shifts of the low-energy constants, $\delta c_1 = -0.13\,\text{GeV}^{-1}$ and $\delta c_3 = 0.89\,\text{GeV}^{-1}$ [15] of the N^{2}LO 3N forces, plus a smaller contribution. The resulting energy of about $-1.5\,\text{MeV}$ per particle at saturation density n_0 in Fig. 2 is $\sim 1/3$ of the N^{2}LO 3N energy, as expected based on the chiral EFT power counting. In contrast, the two-pion–one-pion-exchange 3N force contributions, which include 14 diagrams, are relatively large with $-3.6\,\text{MeV}$ per particle at saturation density. Of similar, but opposite size are the pion-ring 3N force contributions, with $+3.3\,\text{MeV}$ per particle at n_0. The shorter-range parts of N^{3}LO 3N forces depend on the momentum-independent NN contacts, C_T and C_S, which we take consistently from the N^{3}LO EM/EGM potential used. The contributions from the two-pion-exchange–contact 3N forces include 11 diagrams and depend only on C_T. The resulting energy ranges from -2.8 to $+1.3\,\text{MeV}$ at n_0 depending on the NN potential used. These larger 3N results at N^{3}LO are consistent with contributions from the large c_i constants at N^{4}LO exactly in these three topologies [18]. This shows that higher-order many-body forces still need to be investigated and that a chiral EFT with explicit Δ excitations may be more efficient, since this would capture these effects already at N^{3}LO. Finally, the relativistic-corrections 3N forces depend also on $\bar{\beta}_8$ and $\bar{\beta}_9$ [16] and contribute at the few hundred keV level.

The 4N force contributions in Fig. 2 are an order of magnitude smaller than those from the N^{3}LO 3N forces and of similar size as the 3N relativistic corrections. We follow the 4N force notation V^a through V^n of Ref. [17], and include the direct and all 23 exchange terms. Due to the spin-isospin structure, only 3 topologies contribute to neutron matter: the three-pion-exchange 4N forces V^a and V^e, and the pion-pion-interaction 4N forces V^f. The 4N forces V^k and V^n involving the contact C_T vanish in neutron matter due to their spin structure. We find a total 4N force contribution of $-174 \pm 10\,\text{keV}$ per particle at n_0. The V^e and V^f energies largely cancel [19], and their sum agrees with the very small $\sim -20\,\text{keV}$ per particle at n_0 of Ref. [20], which considered these two parts.

Since diagrams beyond Hartree-Fock involving NN interactions and N^{2}LO 3N forces (in particular with the larger c_i at N^{3}LO 3N and without RG evolution) provide non-negligible contributions [2], we include all such diagrams to second order, as well as particle-particle diagrams to third order, which is technically possible based on Ref. [7]. In addition to using NN potentials with different cutoffs and varying the 3N/4N cutoffs, we include estimates of the theoretical uncertainties of the c_i constants and in the convergence of the many-body calculation. The latter is probed by studying the sensitiv-
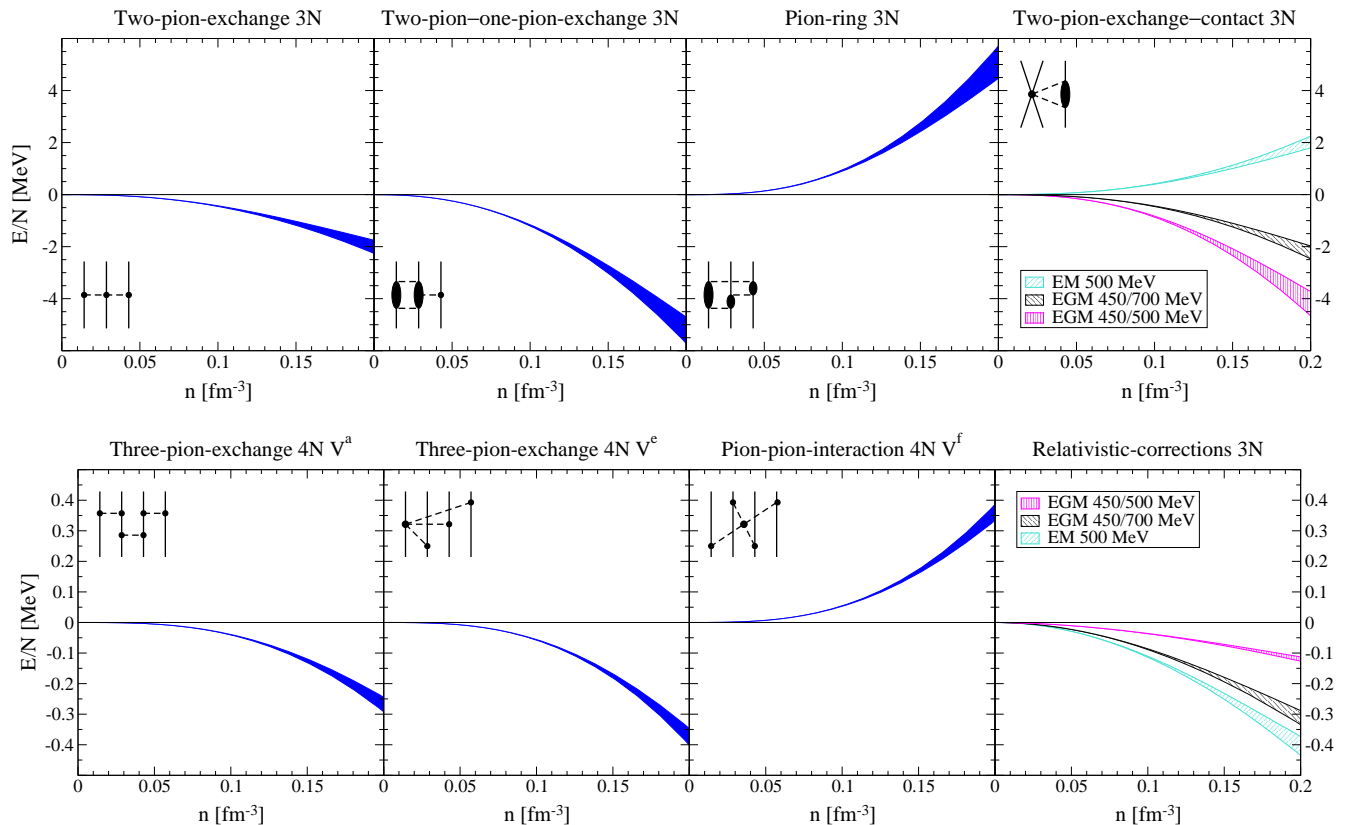
FIG. 2. (Color online) Energy per particle versus density for all individual N³LO 3N and 4N force contributions to neutron matter at the Hartree-Fock level. The bands are obtained by varying the 3N/4N cutoff $\Lambda = 2 - 2.5 \, \text{fm}^{-1}$. For the two-pion-exchange–contact and the relativistic-corrections 3N forces, the different bands correspond to the different NN contacts, C_T and C_S, determined consistently for the N³LO EM/EGM potentials. The inset diagram illustrates the 3N/4N force topology.

ity of the energy to the single-particle spectrum used. We find that the energy changes from second to third order, employing a free or Hartree-Fock spectrum, by $0.8, 0.4, 1.3 \, \text{MeV}$ $(1.4, 0.9, 2.7 \, \text{MeV})$ per particle at $n_0/2$ (n_0) for the EGM 450/500, 450/700, EM 500 N³LO potentials, respectively. The results, which include all these uncertainties, are displayed by the bands in Fig. 1. Understanding the cutoff dependence and developing improved power counting schemes remain important open problems in chiral EFT [21]. For the neutron matter energy at n_0, our first complete N³LO calculation yields $14.1 - 21.0 \, \text{MeV}$ per particle. If we were to omit the results based on the EM 500 N³LO potential, as it converges slowest at n_0, the range would be $14.1 - 18.4 \, \text{MeV}$.

As we find relatively large contributions from N³LO 3N forces, it is important to study the EFT convergence from N²LO to N³LO. This is shown in Fig. 3 for the EGM potentials (N²LO is not available for EM), where the N³LO results are found to overlap with the N²LO band across a $\pm 1.5 \, \text{MeV}$ range around $17 \, \text{MeV}$ at saturation density. As expected from the net-attractive N³LO 3N contributions in Fig. 2, the N³LO band yields lower energies. For the N²LO band, we have estimated the theoretical uncertainties in the same way, and the neutron matter energy ranges from $15.5 - 21.4 \, \text{MeV}$ per particle

at n_0. The theoretical uncertainty is reduced from N²LO to N³LO to $14.1 - 18.4 \, \text{MeV}$, but not by a factor $\sim 1/3$ based on the power counting estimate. This reflects the
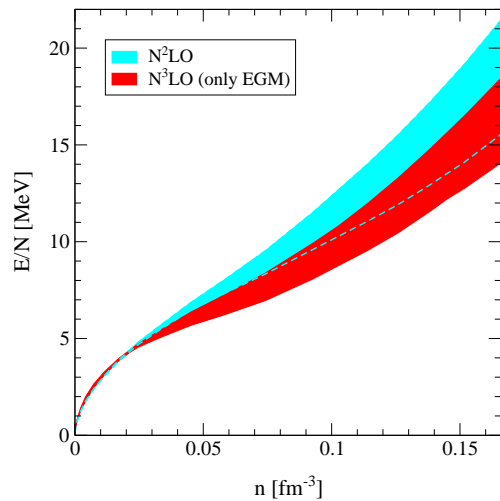

FIG. 3. (Color online) Neutron matter energy per particle as a function of density at N²LO (upper/blue band that extends to the dashed line) and N³LO (lower/red band). The bands are based on the EGM NN potentials and include uncertainty estimates as in Fig. 1.
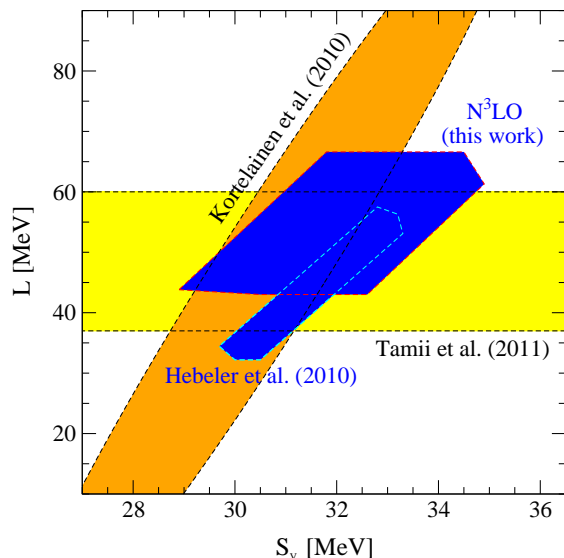
FIG. 4. (Color online) Range for the symmetry energy S_v and its density dependence L obtained at N^3LO (this work) versus including 3N forces at N^2LO (Hebeler *et al.* [8]). For comparison [25], we show constraints obtained from energy-density functionals for nuclear masses (Kortelainen *et al.* [26]) and from the ^{208}Pb dipole polarizability (Tamii *et al.* [27]).

large c_i 3N contributions at N^4LO, and is similar to the convergence pattern observed in chiral NN potentials [1].

The neutron matter energy in Fig. 1 is in very good agreement with NLO lattice results [3] and Quantum Monte Carlo simulations [22] at very low densities (see also the inset) and approximately reproduces the scaling $\sim 0.5 \frac{3k_F^2}{10m}$, which we attribute to effective-range effects combined with low cutoffs [9]. At nuclear densities, we compare our N^3LO results with variational calculations based on phenomenological potentials (APR) [23], which are within the N^3LO band, but do not provide theoretical uncertainties. In addition, we compare the density dependence with results from Auxiliary Field Diffusion MC calculations (GCR) [24] based on nuclear force models adjusted to an energy difference of $32\,\mathrm{MeV}$ between neutron matter and the empirical saturation point. The density dependence is similar to the N^3LO band, but the GCR results are higher below $0.05\,\mathrm{fm}^{-3}$.

The N^3LO band provides key constraints for the nuclear equation of state and for astrophysics. Figure 4 shows, following Ref. [25], the allowed range for the symmetry energy S_v and its density dependence $L = 3n_0\partial_n S_v(n_0)$ (for details on the determination of S_v and L see Ref. [8]). Compared to the results from RG-evolved chiral interactions with 3N forces at N^2LO only [8], we find the same correlation (with the same slope), but not as tight due to the additional density dependences at N^3LO. The N^3LO ranges for S_v and L are $S_v = 28.9 - 34.9\,\mathrm{MeV}$ and $L = 43.0 - 66.6\,\mathrm{MeV}$. The two neutron-matter bands in Fig. 4 are complementary, because the RG evolution in Hebeler *et al.* [8] improves

the many-body convergence, while the band presented in this work is the first consistent N^3LO calculation. The predicted N^3LO range, as well as that of Hebeler *et al.* [8], are in agreement with constraints obtained from energy-density functionals for nuclear masses [26] and from the ^{208}Pb dipole polarizability [27]. In the future, the N^3LO band can be narrowed further by a higher-order many-body calculation with N^3LO 3N forces and by taking into account Δ excitations (explicitly or through large c_i contributions at N^4LO [18]). Combined with the heaviest $2M_\odot$ neutron star [28] and a general extension to high densities [8], our N^3LO energy band leads to a radius range of $R = 9.7 - 13.9$ km for a typical $1.4M_\odot$ neutron star, in remarkable agreement with Ref. [8]. For an alternative determination using in-medium chiral perturbation theory for all densities see Ref. [5].

We have presented the first complete N^3LO calculation of the neutron matter energy, including NN, 3N and 4N forces, with the first application of N^3LO 3N forces to many-body systems. The significant contributions from N^3LO 3N forces show that their inclusion will also be very important for nuclear structure and reactions. Our results provide constraints for the nuclear equation of state and for neutron-rich matter in astrophysics, and highlight the exciting role neutron matter and neutron-rich systems play in chiral EFT, where all many-neutron forces are predicted. The large contributions from N^3LO 3N forces signal the importance of Δ contributions at nuclear densities.

[1] E. Epelbaum, H.-W. Hammer and U.-G. Meißner, Rev. Mod. Phys. **81**, 1773 (2009).
[2] K. Hebeler and A. Schwenk, Phys. Rev. C **82**, 014314 (2010).
[3] E. Epelbaum *et al.*, Eur. Phys. J. A **40**, 199 (2009).
[4] N. Kaiser, S. Fritsch and W. Weise, Nucl. Phys. A **697**, 255 (2002).
[5] W. Weise, Prog. Part. Nucl. Phys. **67**, 299 (2012).
[6] S. K. Bogner, R. J. Furnstahl and A. Schwenk, Prog. Part. Nucl. Phys. **65**, 94 (2010).
[7] K. Hebeler *et al.*, Phys. Rev. C **83**, 031301(R) (2011).
[8] K. Hebeler *et al.*, Phys. Rev. Lett. **105**, 161102 (2010) and in preparation.
[9] A. Schwenk and C. J. Pethick, Phys. Rev. Lett. **95**, 160401 (2005).
[10] S. K. Bogner *et al.*, Nucl. Phys. A **763**, 59 (2005).
[11] E. Epelbaum, W. Glöckle and U.-G. Meißner, Eur. Phys. J. A **19**, 401 (2004); Nucl. Phys. A **747**, 362 (2005).

[12] D. R. Entem and R. Machleidt, Phys. Rev. C **68**, 041001(R) (2003); Phys. Rept. **503**, 1 (2011).

[13] For the EGM $\Lambda/\widetilde{\Lambda} = 550/600$ MeV potential, this is the case only with the larger c_i in 3N forces at N^{3}LO.

[14] S. Ishikawa and M. R. Robilotta, Phys. Rev. C **76**, 014006 (2007).

[15] V. Bernard *et al.*, Phys. Rev. C **77**, 064004 (2008).

[16] V. Bernard *et al.*, Phys. Rev. C **84**, 054001 (2011).

[17] E. Epelbaum, Phys. Lett. B **639**, 456 (2006).

[18] H. Krebs, A. Gasparyan and E. Epelbaum, Phys. Rev. C **85**, 054006 (2012).

[19] H. McManus and D. O. Riska, Phys. Lett. **92B**, 29 (1980).

[20] S. Fiorilla, N. Kaiser and W. Weise, Nucl. Phys. A **880**, 65 (2012).

[21] A. Nogga, R. G. E. Timmermans and U. van Kolck, Phys. Rev. C **72**, 054006 (2005).

[22] A. Gezerlis and J. Carlson, Phys. Rev. C **81**, 025803 (2010).

[23] A. Akmal, V. R. Pandharipande and D. G. Ravenhall, Phys. Rev. C **58**, 1804 (1998).

[24] S. Gandolfi, J. Carlson and S. Reddy, Phys. Rev. C **85**, 032801(R) (2012).

[25] J. M. Lattimer and Y. Lim, arXiv:1203.4286.

[26] M. Kortelainen *et al.*, Phys. Rev. C **82**, 024313 (2010).

[27] A. Tamii *et al.*, Phys. Rev. Lett. **107**, 062502 (2011).

[28] P. B. Demorest *et al.*, Nature **467**, 1081 (2010).